Academic Journal of Science and Technology
ISSN: 2771-3032 | Vol. 10, No. 1, 2024

Rainbow Capture Based on Underwater Gradient Phononic Crystals

Jialin Zhong

School of Physics and Optoelectronic Engineering, Guangdong University of Technology, Guangzhou 510006, People's Republic of China

Abstract: Waves of different frequencies are located and captured at different positions, giving rainbow capture a wide range of potential applications in filtering, buffering, energy collection, and other fields. In this paper, we design a rainbow capture structure based on gradient phonon crystals. The edge states change due to the different structural parameters. By designing a gradient structure, the sound waves of different frequencies are separated and trapped at different boundary positions to form the acoustic rainbow effect. Incident waves from different directions produce significantly distinct rainbow trapping effect. The distance sound propagates when excited from the left is increasingly further, while the distance when excited from the right is increasingly shorter. Besides, the symmetrical rainbow effect has also been demonstrated in symmetrical gradient phonon crystals. This work provides a theoretical reference for achieving diverse multiwavelength devices in acoustic systems.

Keywords: Edge states; rainbow trapping; phononic crystal; underwater structure.

1. Introduction

In recent years, acoustic artificial microstructures, such as phonon crystals and acoustic metamaterials, have been extensively studied for their superior acoustic control characteristics and advanced mechanical properties, and a lot of breakthrough achievements have been made in vibration and noise control[1], sound absorption and insulation[2,3], sound sensors[4], topological sound[5] and sound waveguides[6]. Similar to photonic crystals, the most important property of phonon crystals is the presence of the elastic band gap. The transmission of elastic or acoustic waves within the band gap will be prohibited.[7,8] Phonon crystals have a very broad application prospect and can be used in the design and manufacture of various acoustic devices and systems, such as acoustic lenses[9], acoustic cloaks[10], acoustic isolators[11], acoustic logic gates[12], acoustic sensors[13], acoustic waveguides[14], etc. Phonon crystals can also be combined with research in other fields, such as topological properties[15], nonlinear effects[16], controllability[17], etc., to generate new acoustic effects and functions, providing new solutions and services for technological advances and social needs in the field of acoustics.

The rainbow effect refers to the use of material or structure dispersion to slow down the waves speed and eventually the waves of different frequencies stop at different locations, resulting in the waves of different frequencies being separated in space[18]. For visible light, it is like a "rainbow" that appears in the sky after a rain. Rainbow devices, which have a wide range of potential applications in device multiplexing[19], energy storage[20], and energy focusing[21], have attracted a lot of interest. The means of realizing the rainbow is by gradually changing one or more structural parameters (e. g, position, size, and refractive index.etc) along the direction of propagation. A number of methods for rainbow capture have been proposed, including the use of plasmonic structures[22], nanowires[23], metamaterials[24], metasurfaces[25,26], magneto-optical material waveguides[27,28], and photonic crystal waveguides[29,30], etc. Despite the observation of acoustic rainbow capture in air, the exploration of rainbow capture of elastic waves in the environment of water remains absent.

Here ,we propose a device for capturing rainbows in water. The structural parameters controlling the scatterer rotation affect the band gap size of phonon crystals. Over a certain angular range, the frequencies of the edge states increase monotonically with the increase in rotation angle, allowing the construction of an angularly graded phononic crystal for achieving the rainbow effect. Different from previous structures formed by splicing together phonon crystals of different properties, the structure is a progressively deformed honeycomb-type gradient phononic crystal. In addition, through deliberate structural design, sound waves in symmetrical directions propagate farther and farther with increasing frequency. Our work will promote the further development of sound flow control in water or ocean systems.

2. Structural Design and Calculation Model

In this work, we propose the realization of an underwater acoustic rainbow effect based on two-dimensional phononic crystal. The phononic crystal considered here is a honeycomb lattice composed of six "artificial atoms" arrays, consisting of crescent-shaped rods surrounded by water. The construction of the crescent-shaped rods is shown on the left side of Fig. 1 (a). Consider two cylindrical rods with radius $R = 0.1 \times a$. We regard the crescent-shaped region formed by the overlapping of the two cylindrical rods as the scatterer, as shown in the gray part of Fig. 1 (a), where the displacement distance of the two cylindrical rods is d, where $d = R$. a_1 and a_2 are the lattice vectors with the lattice constant $a = 43\,mm$. Besides, $r = a/3$ is the distance between the unit cell center and the center of the crescent-shaped rod. The crescent-shaped rods rotate around the center of the unit cell six times, each time by $\pi/3$. Thus the system composed of the unit cell of the crescent rod has C_6 rotation symmetry and the double Dirac points in this system are generated by accident. Throughout this work, the commercial software COMSOL Multiphysics is employed to implement numerical simulations.

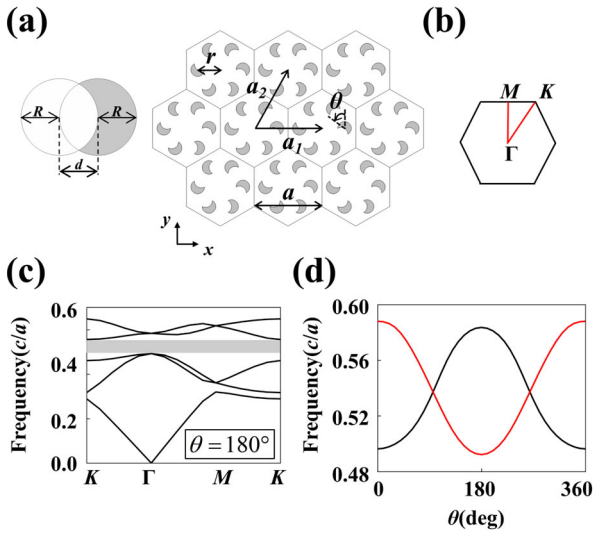

Figure 1. (a) Schematic diagram of the unit cell of the two-dimensional photonic crystal; (b) The first Brillouin zone with high symmetry points; (c) The energy band structure of the unit cell for $\theta = 180°$; (d) The variation of eigenfrequencies with θ.

The material of the scatterers is the soft rubber (gray area) with $\rho_{rubber} = 1000kg/m^3$, $c_{rubber} = 489.9m/s$, while the parameters of the water-based medium are $\rho_{water} = 1000kg/m^3$, $c_{water} = 1482.9m/s$, respectively. The six crescent-shaped rods in the crystal rotate θ by orienting counterclockwise around their respective centers, as shown in Fig. 1 (a). It is observed that the oriented rotation angles of the crescent-shaped rods allow the unit cell to have different configurations. Therefore, we can change the angular orientation by introducing different degrees of angular perturbations to break the spatial inversion symmetry, which will open the bandgap at the Γ point. In order to simplify the calculation and effectively display the main characteristics of the band, we calculate the band structure along the path of the high symmetric point (Fig. 1 (b)) in the Brillouin zone, as shown in Fig. 1 (c). The bandgap is displayed by shaded areas. All frequencies in the graph have been normalized. The eigenfrequency of the Γ point at the center of the Brillouin zone varies with the rotation angle θ in Fig. 1 (d). We only consider $\theta \in [0°, 360°]$, the rotation period of the scatterer. For $\theta = 0°$ and $\theta = 180°$, the bandgap is opened. The energy bands are doubly degenerate at the Γ point, and the upper and lower edges of the bandgap are a function of the rotation angle θ.

3. Dispersion Analysis

It can be seen from the band structure of the unit cell that the rotation angle θ plays an important role in controlling the band gap of phonon crystals. Next, we investigate the projected dispersion of the supercell circled by the blue dashed line in Fig. 2 (a). This boundary situation preserves the symmetry of the crystal, reducing the coupling between the counter-propagating modes. The supercell structure is periodic in the k_x direction and finite in the k_y direction. Different from the dispersion of the recent researches[31,32], the supercell is not composed of two different phonon crystals. The edge state dispersion in the band gap is shown in Fig. 2 (b), with the upper and lower edge states represented in blue and red respectively. Since the upper and lower boundary condition cases are the same, the two edge states are almost degenerate. However, we only focus on the upper edge states (the blue curve) in the following discussion.

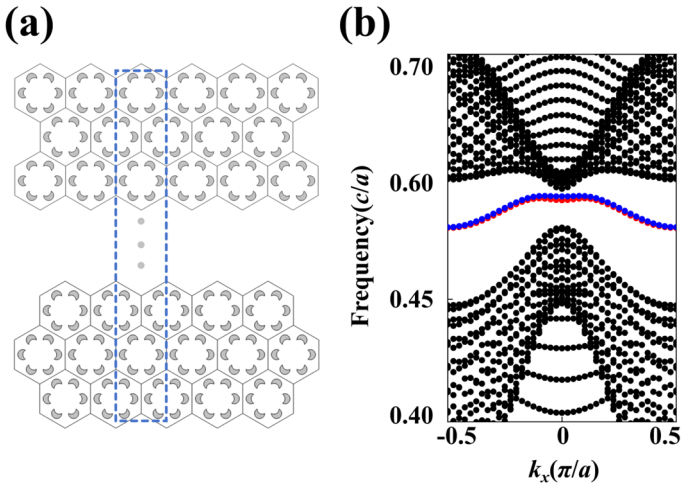

Figure 2. (a) Schematic diagram of supercell structure with $\theta = 0°$; (b) The edge state of the super unit cell demonstrated by the blue dashed frame in (a).

By changing the rotation angle θ, we calculate the dispersion curves and the corresponding group velocities of the supercell at different angles. As shown in Fig. 3 (a), the frequencies of the dispersion curves increase monotonically with the parameter θ changing from 120° to 170° in the range of normalized frequency $0.5c/a$ to $0.58c/a$. Correspondingly, the low group velocity ($c < 1$) is obtained as shown in Fig. 3 (b). The trend is that both the dispersion curve and the corresponding low group velocity move to the high frequency with the increase of θ. It can be seen from the separated dispersion curve that acoustic waves of different frequencies propagate at different group velocities along the edge state. When the group velocity of the acoustic wave decreases to zero in the direction of propagation, the wave is not allowed to propagate. Therefore, the dispersion property allows the separation of modes of different frequencies and the capture of sound waves at specific locations.

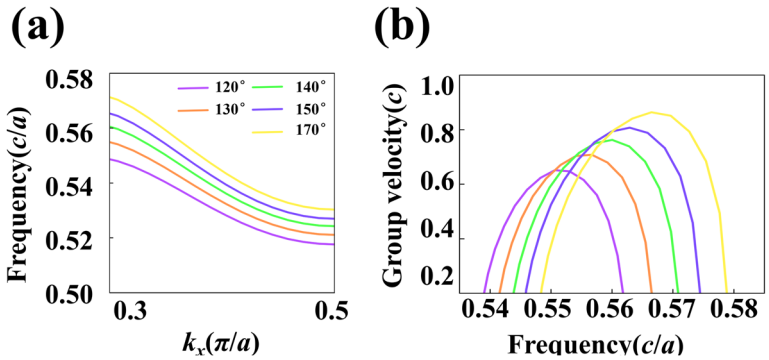

Figure 3. (a) The dispersion curve of the edge state of the supercell with parameter $\theta = 120°$, $\theta = 130°$, $\theta = 140°$, $\theta = 150°$, $\theta = 170°$; (b) The calculated group velocity corresponds to (a)

4. Rainbow Structure Design

By using the frequency shift of the edge states and group velocities in different angles, rainbow structures can be designed on purpose. This property is the key principle of rainbow effect. Here, we consider the frequency range of the band gap, where sound waves can only travel along the boundary. In order to investigate the rainbow effect, we design a finite structure composed of supercells as shown in Fig 4 (a). The rotation angle is spatially modulated by equation (1). We define that the rotation angle of the n-th column along the x direction in the 2D phononic crystal structure is represented by the parameter $\theta(n)$:

$$\theta_{(n)} = \theta_0 + \frac{\theta_m - \theta_0}{m-1} \times (n-1), 1 < n < m \qquad (1)$$

Where, θ_1 and θ_m are the rotation parameters of the first column and last column .Obviously, the spatial modulation leads the phononic crystals in each column to rotate at a particular angle. For our acoustic system, $m = 19$. The angle of rotation increases as the number of columns gradually increases and $\theta_0 = 90°$ and $\theta_m = 180°$, respectively. In other words, the angle of the gradient phononic crystal increases monotonically from 90° (the first column, on the far left) to 180° (the last column, on the far right) along the θ-axis. The rotation increment is $\Delta\theta = 5°$. If the spatial modulation of θ is ideally smooth and slow enough, the structure is locally equivalent to the phononic crystal model in Fig 2 (a). The change in rotation angle is very small.

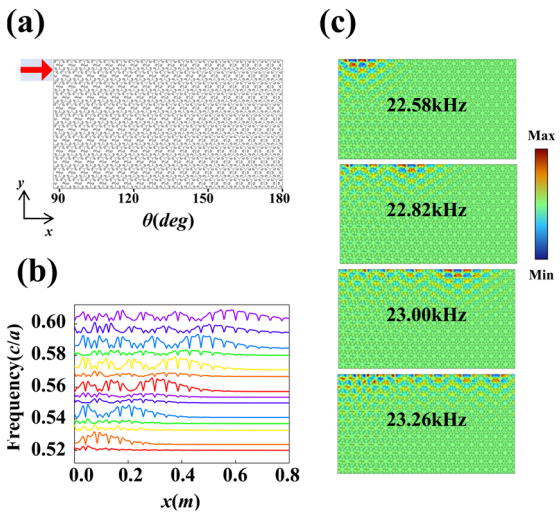

Figure 4. (a) Schematic of the gradient phononic crystal waveguide with adjusting θ parameters for realizing the rainbow capture; (b) Acoustic pressure distributions along the upper boundary when left incidence; (c) The sound pressure field corresponding to different frequencies.

After constructing the phonon crystal gradient structure, we add excitation from different directions. The red arrow in Fig. 4 (a) illustrates the incidence of sound waves from the left side of the upper boundary. The normalized intensity distribution along the boundary within a certain frequency range is shown in Fig. 4 (b). The specific distributions of sound pressure fields with incident frequencies of $22.58kHz$, $22.82kHz$, $23.00kHz$ and $23.26kHz$ are shown in Fig. 4 (c). Specifically , when excited from left, the acoustic waves propagate to the right along the boundary, and the acoustic waves propagate progressively further away from each other as the frequency of excitation rises. The results indicate that acoustic waves of different frequencies stop at different positions. As the acoustic waves propagate forward, the energy of the acoustic field progressively spreads farther with increasing excitation frequency. The results unequivocally demonstrate that our gradient phonon crystal structure effectively realizes the rainbow effect.

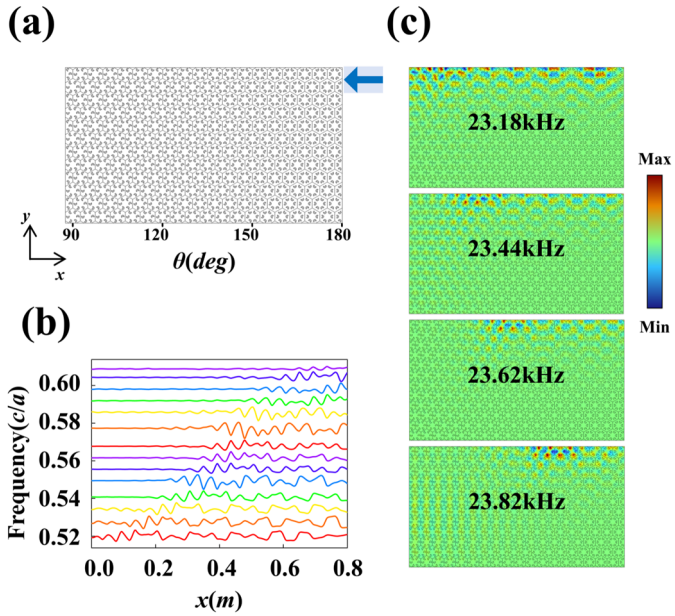

Figure 5. (a) Schematic of the gradient phononic crystal waveguide with adjusting θ parameters for realizing the rainbow capture; (b) Acoustic pressure distributions along the upper boundary when right incidence; (c) The sound pressure field corresponding to different frequencies.

Correspondingly, the blue arrow in Fig. 5 (a) illustrates the incidence of sound waves from the right side. As shown in Fig. 5 (b), the sound pressure intensity along the boundary gradually approaches the sound source as the frequency increases. The specific distributions of sound pressure fields with incident frequencies of $23.18kHz$, $23.44kHz$, $23.62kHz$ and $23.82kHz$ are shown in Fig. 5 (c), indicating that acoustic waves of different frequencies propagate progressively closer as the frequency increases. It is worth noting that these two different rainbow effects are produced in the same gradient phonon crystal structure, with the rotation angle gradually increasing from the first to the last column. The difference between this case and Fig. 4 lies in the direction of the incident wave, which results in a different rainbow effect related to the design of the gradient structure.

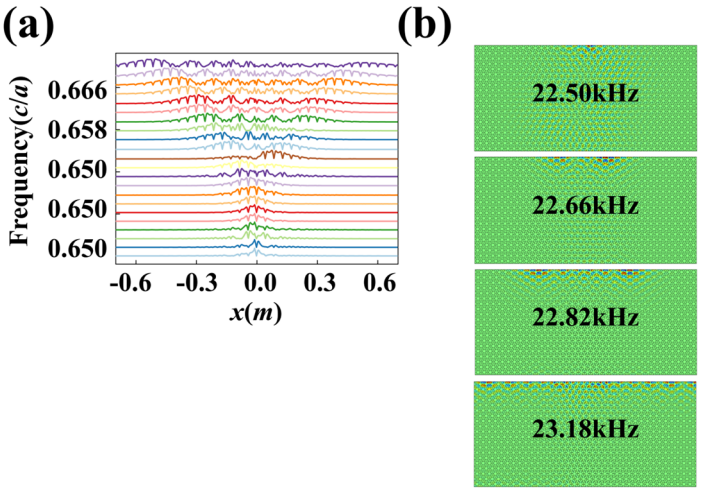

Figure 6. (a) Acoustic pressure distributions along the upper boundary when middle incidence; (b) The sound pressure field corresponding to different frequencies.

In addition, we construct a gradient phononic crystal with central mirror symmetry based on Fig. 4 and Fig. 5. Similar to the results above, the acoustic waves propagate progressively further away the source along the boundary. Fig. 6 (a) depicts the propagation distance of sound waves at different frequencies. The sound pressure fields with incident frequencies of $22.50kHz$, $22.66kHz$, $22.82kHz$ and $23.18kHz$ are shown in Fig. 6 (b). It can be observed that as the rotation angle increases, the frequencies of the edge state also increase, resulting in a progressively longer propagation distance along the boundary. This phenomenon validates the successful realization of the rainbow structure, thereby offering a novel approach towards achieving a multi-directional underwater rainbow effect.

5. Summary

In conclusion, this letter investigates the acoustic rainbow effect based on the design of gradient two-dimensional phononic crystal structures. The structure-dependent rotation parameter θ is used to open the bandgap and generate the edge states. By choosing the appropriate rotation angle, the gradient structure is artfully designed. The simulation results demonstrate that the sound waves with different incident directions produce the different rainbow effects, which are determined by the inherent property of the gradient structure. Furthermore, we also verify the symmetric transmission of sound rainbow capture in the simulation. This work may provide a new reference for the transmission and manipulation of sound waves in water.

References

[1] Lilly, J.G. Mechanical noise and vibration control. The Journal of the Acoustical Society of America 2021, 150, A23-A23, doi:10.1121/10.0007495.

[2] Zhang, X.H.; Qu, Z.G.; Tian, D.; Fang, Y. Acoustic characteristics of continuously graded phononic crystals. Applied Acoustics 2019, 151, 22-29, doi:https://doi.org/10.1016/j.apacoust.2019.03.002.

[3] Zhang, X.; Qu, Z.; Xu, Y. Enhanced sound absorption in two-dimensional continuously graded phononic crystals. Japanese Journal of Applied Physics 2019, 58, 090904, doi:10.7567/1347-4065/ab3686.

[4] Dong, Q.; Liu, H. A bio-inspired sound source localization sensor with internal coupling. The Journal of the Acoustical Society of America 2019, 145, 1864-1864, doi:10.1121/1.5101734.

[5] Yves, S.; Ni, X.; Alù, A. Topological sound in two dimensions. Annals of the New York Academy of Sciences 2022, 1517, 63-77, doi:https://doi.org/10.1111/nyas.14885.

[6] Cselyuszka, N.; Alù, A.; Janković, N. Spoof-Fluid-Spoof Acoustic Waveguide and its Applications for Sound Manipulation. Physical Review Applied 2019, 12, 054014, doi:10.1103/PhysRevApplied.12.054014.

[7] Wu, F.; Liu, Z.; Liu, Y. Acoustic band gaps created by rotating square rods in a two-dimensional lattice. Physical Review E 2002, 66, 046628, doi:10.1103/PhysRevE.66.046628.

[8] Jia, Z.; Bao, Y.; Luo, Y.; Wang, D.; Zhang, X.; Kang, Z. Maximizing acoustic band gap in phononic crystals via topology optimization. International Journal of Mechanical Sciences 2024, 270, 109107, doi:https://doi.org/10.1016/j.ijmecsci.2024.109107.

[9] Zhang, X.; Li, W.; Zeng, Z.; Wang, Z. Simple broadband planar acoustic lenses design with a velocity gradient structure. Applied Acoustics 2024, 217, 109832, doi:https://doi.org/10.1016/j.apacoust.2023.109832.

[10] Zhang, H.; He, J.; Liu, C.; Ma, F. A wideband acoustic cloak based on radar cross section reduction and sound absorption. Applied Acoustics 2023, 213, 109639, doi:https://doi.org/10.1016/j.apacoust.2023.109639.

[11] Zhang, H.; Li, R.; Bao, Y.; Liu, X.; Zhang, Y. Total acoustic transmission in a honeycomb network empowered by compact acoustic isolator. Scientific Reports 2023, 13, 828, doi:10.1038/s41598-023-28097-y.

[12] Li, Y.; Huang, K.; Gong, M.; Sun, C.; Gao, S.; Lai, Y.; Liu, X. Realization of acoustic tunable logic gate composed of soft materials. Results in Physics 2024, 57, 107421, doi:https://doi.org/10.1016/j.rinp.2024.107421.

[13] Kabir, M.; Kazari, H.; Ozevin, D. Piezoelectric MEMS acoustic emission sensors. Sensors and Actuators A: Physical 2018, 279, 53-64, doi:https://doi.org/10.1016/j.sna.2018.05.044.

[14] Esfahlani, H.; Byrne, M.S.; McDermott, M.; Alù, A. Acoustic Supercoupling in a Zero-Compressibility Waveguide. Research 2019, doi:10.34133/2019/2457870.

[15] Chen, C.; Chen, T.; Ding, W.; Yang, F.; Zhu, J.; Yao, J. Impurity-induced multi-bit acoustic topological system. International Journal of Mechanical Sciences 2023, 247, 108183, doi:https://doi.org/10.1016/j.ijmecsci.2023.108183.

[16] Abily, T.; Regnard, J.; Gabard, G.; Durand, S. Non-linear effects in thin slits for low frequency sound absorption. Journal of Sound and Vibration 2023, 546, 117432, doi:https://doi.org/10.1016/j.jsv.2022.117432.

[17] Pan, S.; You, R.; Chen, X.; Pan, W.; Li, Q.; Chen, X.; Pang, W.; Duan, X. Regulating Biomolecular Surface Interactions Using Tunable Acoustic Streaming. ACS Sensors 2023, 8, 3458-3467, doi:10.1021/acssensors.3c00982.

[18] Kosmas, L.T.; Ortwin, H. Slow and stopped light in metamaterials: the trapped rainbow. In Proceedings of the Proc.SPIE, 2008; p. 698702.

[19] Zhong, Z.; Liu, T.; Wu, H.; Qiu, J.; Du, B.; Yin, G.; Zhu, T. High-spatial-resolution distributed acoustic sensor based on the time-frequency-multiplexing OFDR. Opt. Lett. 2023, 48, 5803-5806, doi:10.1364/OL.501253.

[20] Tian, Y.-Z.; Tang, X.-L.; Wang, Y.-F.; Laude, V.; Wang, Y.-S. Annular acoustic impedance metasurfaces for encrypted information storage. Physical Review Applied 2023, 20, 044053, doi:10.1103/PhysRevApplied.20.044053.

[21] Gao, N.; Wu, J.H.; Yu, L.; Hou, H. Ultralow frequency acoustic bandgap and vibration energy recovery in tetragonal folding beam phononic crystal. International Journal of Modern Physics B 2016, 30, 1650111, doi:10.1142/S0217979216501113.

[22] Ghaderian, P.; Habibzadeh-Sharif, A. Rainbow trapping and releasing in graded grating graphene plasmonic waveguides. Opt. Express 2021, 29, 3996-4009, doi:10.1364/OE.414982.

[23] Hussein, M.; Hameed, M.F.O.; Areed, N.F.F.; Yahia, A.; Obayya, S.S.A. Funnel-shaped silicon nanowire for highly efficient light trapping. Opt. Lett. 2016, 41, 1010-1013, doi:10.1364/OL.41.001010.

[24] Xu, J.; Xiao, S.; He, P.; Wang, Y.; Shen, Y.; Hong, L.; Luo, Y.; He, B. Realization of broadband truly rainbow trapping in gradient-index metamaterials. Opt. Express 2022, 30, 3941-3953, doi:10.1364/OE.447874.

[25] Xu, Z.; Shi, J.; Davis, R.J.; Yin, X.; Sievenpiper, D.F. Rainbow Trapping with Long Oscillation Lifetimes in Gradient Magnetoinductive Metasurfaces. Physical Review Applied 2019, 12, 024043, doi:10.1103/PhysRevApplied.12.024043.

[26] Liu, T.; Liang, S.; Chen, F.; Zhu, J. Inherent losses induced absorptive acoustic rainbow trapping with a gradient metasurface. Journal of Applied Physics 2017, 123, 091702, doi:10.1063/1.4997631.

[27] Xu, J.; He, P.; Feng, D.; Yong, K.; Hong, L.; Shen, Y.; Zhou, Y. Slow wave and truly rainbow trapping in a one-way terahertz waveguide. Opt. Express 2021, 29, 11328-11341, doi:10.1364/OE.422274.

[28] Liu, K.; He, S. Truly trapped rainbow by utilizing nonreciprocal waveguides. Scientific Reports 2016, 6, 30206, doi:10.1038/srep30206.

[29] Sharma, S.; Mondal, A.; Das, R. Infrared rainbow trapping via optical Tamm modes in an one-dimensional dielectric chirped photonic crystals. Opt. Lett. 2021, 46, 4566-4569, doi:10.1364/OL.437958.

[30] Baba, T.; Mori, D.; Inoshita, K.; Kuroki, Y. Light localizations in photonic crystal line defect waveguides. IEEE Journal of Selected Topics in Quantum Electronics 2004, 10, 484-491, doi:10.1109/JSTQE.2004.829201.

[31] Wu, L.-H.; Hu, X. Scheme for Achieving a Topological Photonic Crystal by Using Dielectric Material. Physical Review Letters 2015, 114, 223901, doi:10.1103/PhysRevLett.114.223901.

[32] He, C.; Ni, X.; Ge, H.; Sun, X.-C.; Chen, Y.-B.; Lu, M.-H.; Liu, X.-P.; Chen, Y.-F. Acoustic topological insulator and robust one-way sound transport. Nature Physics 2016, 12, 1124-1129, doi:10.1038/nphys3867.